Porous ZnO nanosheets with multichromic conducting polymer core/shell composite: enhanced electrochromic performances

Journal:	*New Journal of Chemistry*
Manuscript ID:	NJ-ART-11-2013-001407.R2
Article Type:	Paper
Date Submitted by the Author:	24-Feb-2014

Complete List of Authors:	Lv, Xiaojing; Zhejiang University of Technology, Sun, JingWei; Zhejiang University of Technology, Wang, Pingjing; Zhejiang University of Technology, Wu, Qichao; Zhejiang University of Technology, Ouyang, Mi; Zhejiang University of Technology, Huang, Senbiao; Zhejiang University of Technology, Yang, Yuan; Zhejiang University of Technology, Zhang, Cheng; Zhejiang University of Technology, College of Chemical Engineering and Materials Science

Journal Name

RSCPublishing

ARTICLE

Porous ZnO nanosheets with multichromic conducting polymer core/shell composite: enhanced electrochromic performances

Xiaojing Lv, Jingwei Sun, Pingjing Wang, Qichao Wu, Mi Ouyang*, Senbiao Huang, Yuan Yang and Cheng Zhang*

Cite this: DOI: 10.1039/x0xx00000x

Received 00th January 2012,
Accepted 00th January 2012

DOI: 10.1039/x0xx00000x

www.rsc.org/

Porous ZnO nanosheets with multichromic conducting polymer -poly(4,4',4"-tris[4-(2-bithienyl)pheny]amine) (PTBTPA) core/shell composite were prepared by electrodeposition combining with electropolymerization method. The composite film exhibits noticeable electrochromism with reversible color changes from orange, olive green in to dark gray. An optical contrast of 68.7% and a switching time of 0.96 s are obtained for the composite film, better than that of the pure PTBTPA film, 51.8% and 1.95 s. The cyclic stability studies reveal that the composite film exhibits much more enhanced durability and retains 70% of the electroactivity even after 1000 cycles. However, the pure PTBTPA film loses almost most of its electroactivity after 1000 cycles. The core/shell composite structure is believed to be responsible for the observed enhanced electrochromic performance. On one hand, porous ZnO nanosheets with loose inner space can facilitate counterions into the polymer film and shorten the diffusion distance, devoting to the higher optical contrast and faster switching speed; on the other hand, the larger contact area can enhance the adhesion between the polymer and the ITO electrode, contributing to better electrochemical stability.

1. Introduction

Conducting polymers (CPs) based electrochromic (EC) materials have been widely studied owing to their good processibility, diverse colors and high optical contrast [1-6] for various applications, such as smart window, reflectance mirrors, thin flat panel displays and memory devices [7-10]. Apart from multicolor-displaying, fast switching rate and good electrochemical stability are the most two essential factors for EC materials for the practical applications. However, it is difficult for the pure CPs-based EC materials to realize the two properties. Organic/inorganic nanocomposite materials are emerging as new class of EC materials to improve the performances for the prime reasons that they could often combine the mulichromic behavior of organic polymers and the high thermal and chemical stability followed by the inorganics, which may offer special properties through the reinforcement or modification of each other [11, 12]. Several groups have demonstrated that such nanocomposites can exhibit faster switching speed and better stability than the corresponding polymer. Sonavane et. al [13, 14] reported NiO/PPy and NiO/PANI composite films with improved coloration efficiency and electrochemical stability. Zhu et. al [15] reported that electrical switching and high contrast ratio of poly(p-phenylenebenzobisthiazole) (PBZT) thin films were enhanced by embedding with WO_3 nanoparticles. Wei et. al [16, 17] incorporated WO_3 and GO nanoparticles into PANI, which could improve the cycling stability of the electrochromic composites. Cai et al. [18, 19] synthesized WO_3/polyaniline and TiO_2/polyaniline core/shell composite films with high coloration efficiency and good cycling stability. Wu et al. [20] observed that, with the addition of TiO_2 nanorods, the optical contrast, coloration efficiency, and stability of poly-(4,4-dioctylcyclopenta[2,1-b:3,4-b']-dithiophene (PDOCPDT) were enhanced significantly. Bae et. al [21] reported that electrochromic contrast, switching time, and coloration efficiency were significantly improved in the hybrid devices consisted of PANI with TiO_2 nanoparticles. Bhandari et. al [22] obtained larger coloring efficiency and faster color-bleach

kinetics of Poly(3,4-ethylenedioxythiophene)-Au-CdSe nanocomposite films. In all of the previously described studies, conducting polymer/inorganic nanocomposite is an efficient way to attain considerable electrochromic performance for practical applications.

Nano-ZnO has been the promising elements for both fundamental research and practical studies because of its good environmental stability, excellent electron transport properties and preferable transparency [23-29]. Electrochromic composites embedded with Nano-ZnO have been rarely reported. Sun et. al [30] firstly designed an electrochromic (EC) display using a viologen-modified ZnO nanowire array as the EC electrode with fast switching time. Recently, Kateb et. al [31] prepared an electrochromic device based on poly(3,4-ethylenedioxythiophene) (PEDOT) modified ZnO nanowires, which exhibited faster switching and higher optical contrast. Our previous work [32] reported that ZnO nanorods/PTBTPA composite film exhibited higher optical contrast, faster response speed and improved electrochemical stability. Therefore, Nano-ZnO is a good candidate for the organic/inorganic nanocomposite materials to improve the EC performance. It inspires us to explore novel nanostructures to combine with the electrochromic polymer and investigate its impact on the electrochromic properties. Porous ZnO nanosheets prepared via electrochemical deposition have been drawn into consideration due to high porosity, large surface area and good film-forming directly on the electrode surface. On one hand, porous ZnO nanosheets with loose inner space and larger contact area can facilitate counterions into the polymer film; on the other hand, the film-forming directly on the substrate via electrochemical route can enhance the adhesion between the polymer and the electrode [33-37]. Therefore, it is expected to obtain more excellent performance with the composite system.

In the present study, we report a core/shell composite of multichromic polymer-poly(4,4',4''-tris[4-(2-bithienyl)pheny]amine) (PTBTPA) incorporating with porous ZnO nanosheets via electrodeposition combining with electropolymerization techniques. Electron micrographs show ZnO nanosheets consist of a great amount of nanoparticles belong to one-dimensional hierarchically nanostructure, which have been rarely used in the composite system. Cyclic voltammogram, UV-vis absorption spectra and electrochemical impedance exhibit the composite film has lower onset oxidative potential, energy band and less electrochemical resistance. Therefore, the composite film presents higher optical contrast, faster switching speed and better electrochemical stability, which is a promising candidate for the EC applications.

2. Experimental

2.1. Chemicals

zinc nitrate hexahydrate ($Zn(NO_3)_2$), potassium sulfate (K_2SO_4), potassium chloride (KCl), tetrabutylammonium perchlorate (TBAP), dichloromethane (DCM), chromatography grade acetonitrile (ACN) were purchased and used as received. The monomer of 4,4',4''-tris[4-(2-bithienyl)pheny]amine (TBTPA) was synthesized according to the ref. [38]. Indium tin oxide (ITO) glass substrates (CSG HOLDING Co., Ltd., $Rs \leq 10\Omega\square^{-1}$, the area: 1 cm × 4 cm) were used by ultrasonic washing in distilled water, ethanol and acetone solutions, respectively.

2.2. Characterization

Surface morphologies and microstructures of PTBTPA film, ZnO nanosheets and PTBTPA/ZnO composite film were investigated by S-4800 scanning electron microscope (SEM) (Hitachi, Japan) and Tecnai G2 F30 S-Twin high resolution transmission electron microscopy (HR-TEM) (Philips-FEI, Holland). The structure characteristic was recorded by a Nicolet 6700 Fourier-transform infrared spectrometer (FTIR) (Thermo Fisher Nicolet, USA). The element analysis of composite film was studied by energy dispersion X-ray spectrum (EDX). The electrochemical properties, including cyclic voltammogram, electrochemical stability and electrochemical impedance measurement were performed in a three-compartment system containing 0.1 M TBAP in DCM/ACN solutions (7: 3, by volume) as the electrolyte on a CHI660C electrochemical analyzer (Chenhua, China). UV-vis absorption spectra, optical contrast and switching time measurement were carried out on a Shimadzu UV-1800 spectrophotometer (Shimadzu, Japan) integrated with CHI660C electrochemical analyzer.

2.3. Synthesis of the composite film

ZnO nanosheets were synthesized on the ITO substrate using electrodeposition method similar to that described previously [39] with slightly modifications. A three-electrode cell system was utilized with ITO substrate as the working electrode, a platinum (Pt) sheet (4 cm^2) as counter electrode and a double-junction Ag/AgCl electrode (silver wire coated with AgCl in saturated KCl solution, 0.1 M KCl aqueous solution as the second junction) as reference electrode, respectively. The electrolyte consisted of 0.1 M $Zn(NO_3)_2$ and 0.01 M K_2SO_4 aqueous solution. Electrodeposition parameters were selected as follows: the temperature controlled at 70 ^oC by immersing the cell into an oil bath, the potential at -1.1V and the time for about 20 s. After electrodeposition, the as-obtained films were heat treated at 650 ^oC for 2 h.

The composite film was prepared via electropolymerization onto the ZnO-coated substrate. The electropolymeriaztion route was outlined in Scheme 1. All the composite films used for characterization and measurement in this study were obtained via the constant potential polymerization of 0.75 mM TBTPA and 0.1 M TBAP in DCM/ACN solutions (7: 3, by volume) at 1.2 V, which were performed in a conventional three compartment electrolysis cell with ZnO-coated ITO substrate (the active area: 1 cm × 3 cm) as working electrode, a platinum (Pt) sheet (4 cm^2) as counter electrode and a double-junction Ag/AgCl electrode (silver wire coated with AgCl in saturated KCl solution, 0.1 M TBAP in DCM/ACN solution as the second junction) as reference electrode. The charge capacity of polymerization was controlled at 4×10^{-2} C.

3. Results and discussion

Porous ZnO nanosheets with multichromic conducting polymer (PTBTPA) core/shell composite film were prepared by electrodeposition combining with electropolymerization method. ZnO nanosheets were synthesized on the ITO substrate in a three-electrode cell system containing 0.1 M $Zn(NO_3)_2$ and 0.01 M K_2SO_4 electrolyte solution. And the composite film was obtained on the ZnO-coated ITO electrode via the constant potential polymerization of 0.75 mM TBTPA and 0.1 M TBAP in DCM/ACN solutions. Fig. 1 shows SEM images of the as-prepared ZnO, PTBTPA film and PTBTPA/ZnO composite film. ZnO presents uniform and well-distributed nanosheets morphology (Fig. 1a). The higher magnification SEM image clearly shows the rough and porous structure in the individual nanosheet with the thickness of about 80 nm and the length of about 0.75 μm (Fig. 1b, 1c). Moreover, the individual nanosheet is composed of small nanoparticles. From Fig. 1d-1f, the nanosheets become thicker and larger with thickness of about 100 nm and the length of about 0.8 μm which indicates that the ZnO nanosheets are coated by a thin layer of PTBTPA film. Therefore, the composite film exhibits a core/shell structure with the core of ZnO nanosheets and the shell of PTBTPA film instead of an integrated film structure. A plausible formation mechanism can be described as follows: ZnO nanosheets consisted of lots of nanoparticles act as a template for PTBTPA growth during the electropolymerization, leading to the preferential growth of PTBTPA along ZnO nanosheets. The nucleation and growth of PTBTPA occurs along the surface of ZnO nanosheets due to the electrostatic interactions. As constantly electropolymerizing, the polymer gradually deposits and covers ZnO nanosheets to form the core/shell structure. The two-level structure of ZnO nanosheets is more favorable for enhancing the adhesion of the polymer on the electrode, which contributes to improve the EC stability.

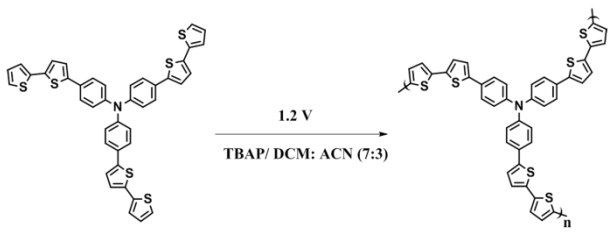

Scheme 1 Electropolymerization route of TBTPA

TEM images of ZnO nanosheets, PTBTPA film and PTBTPA/ZnO composite film are shown in Fig. 2. From the TEM images, it is noticed that they have different surface morphologies. Fig. 2a presents the large ZnO nanosheets are composed of small nanoparticles with the average of 5-10 nm, which is accorded with the SEM images. The high resolution TEM image (Fig. 2b) demonstrates that the d-spacing value of the adjacent lattice planes is 0.2609 nm corresponding to (002) plane of wurtzite hexagonal ZnO crystalline. The pure PTBTPA exhibits a piece of irregular membranous structure with the amorphous character (Fig. 2c). However, it is can be seen the composite film is composed of the inner ZnO layer and the outer polymer layer with a clear interface line (Fig. 2d). The enlarged ZnO layer (Fig. 2e) presents it is consisted of the crystalline ZnO nanoparticles and amorphous polymer. Moreover, the EDX pattern of the composite film contains all the peaks of Zn, C, O, S, N elements of ZnO and PTBTPA compounds. All the results demonstrate the polymer PTBTPA and ZnO nanosheets achieve a fully effective composite.

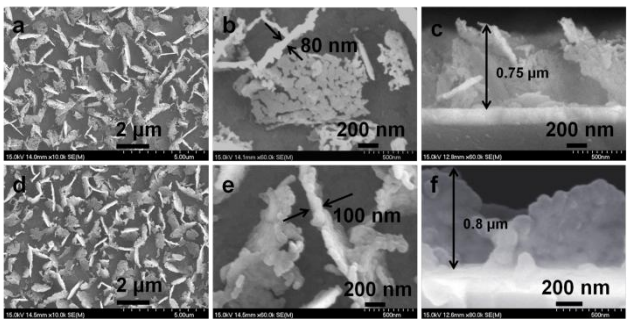

Fig.1 SEM images of ZnO nanosheets and PTBTPA/ZnO composite film (charge: 0.04 C): (a, d) low magnification, (b, e) high magnification, (c, f) cross-section

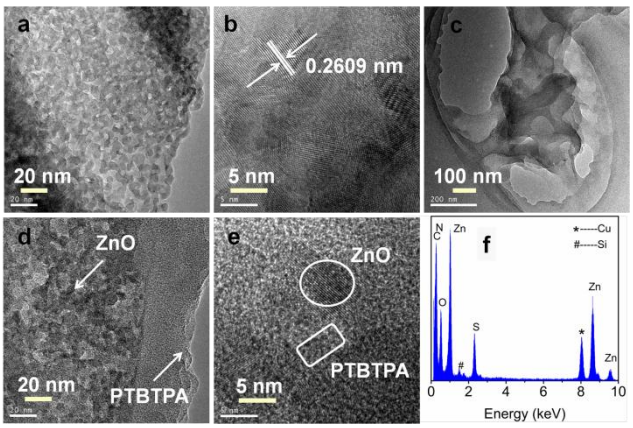

Fig. 2 TEM images and EDX pattern of (a) ZnO nanosheets, (b) ZnO nanosheets (high magnification), (c) PTBTPA film, (d) PTBTPA/ZnO composite film, (f) PTBTPA/ZnO composite film (high magnification), (e) EDX pattern of ZnO nanosheets

Fig. 3 shows the FTIR spectra of the ZnO nanosheets, PTBTPA film and PTBTPA/ZnO composite film. Peaks of PTBTPA at 1600 cm^{-1} should be ascribed to the C-C stretching vibrations in the phenyl ring. The peak at 794 cm^{-1} is the characteristic of C-S bonds in the thiophene rings [40]. The peaks at 1496 and 1427 cm^{-1} are originated from the stretching of thiophene rings [41].The bands at 1315 and 1267 cm^{-1} are due to the C-N vibrations [42]. For ZnO, the strong and wide ad sorption peak at 3328 cm^{-1} is the O-H stretching band on the surface of ZnO [43]. The spectrum of PTBTPA/ZnO composite film contains all the characteristic bands of above two compounds with a little shift. For instance, the band at 1626 cm^{-1} is attributed to the C–C stretching vibrations in the phenyl ring. The peak at 791 cm^{-1} is corresponding to the characteristic of the C-S bonds in the thiophene rings. The bands at 1343 and 1283 cm^{-1} are due to the C-N vibrations. The strong and wide adsorption peak at 3435 cm^{-1} is the O-H stretching band on the

surface of ZnO. Therefore, the similarity of FTIR spectra also demonstrates an effective formation of the PTBTPA/ZnO composite film.

Fig. 4 displays the cycle voltammetry curves of TBTPA in DCM/ACN (7:3, by volume) containing 0.1 M TBAP with ITO and ZnO-coated ITO as working electrode from 0 V to 1.4 V at a scan rate of 100 mVs^{-1}. TBTPA exhibits a couple of reversible redox peaks with the oxidative onset potential at 0.82 V, oxidative peak at 1.07 V and reductive peak at 0.77 V, respectively (Fig. 4a). The oxidation current increased with the increasing scanning cycle, suggesting the deposition of electroactive polymer (PTBTPA) film on ITO electrodes. Fig. 4b shows the similar reversible redox peaks with the oxidative onset potential at 0.71 V, oxidative peak at 0.93 V, reductive peak at 0.68 V and increased oxidation current with the increasing scanning cycle. Obviously, the introduction of ZnO nanosheets into the composite film can decrease the onset oxidative potential of the monomer, indicating that the polymerization reaction is easier to occur on the ZnO-coated electrode than the ITO electrode [44].

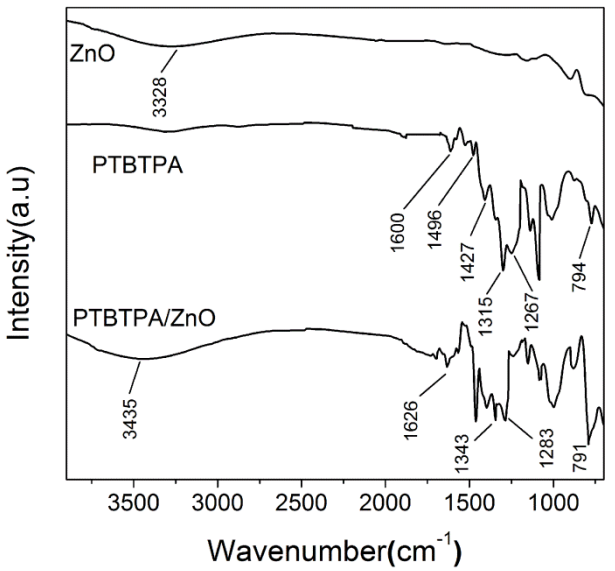

Fig. 3 FT-IR spectra of ZnO nanosheets, PTBTPA film and PTBTPA/ZnO composite film

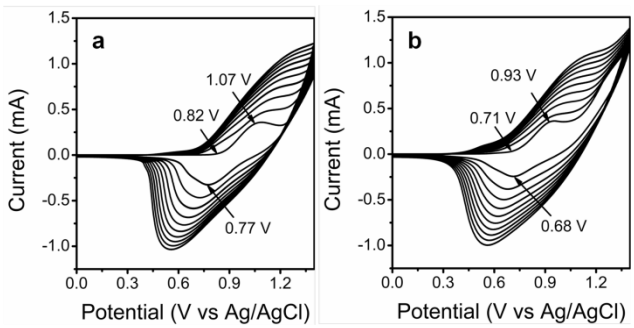

Fig. 4 Cyclic voltammogram curves of 0.75 mM TBTPA in DCM/ACN solutions (7: 3, by volume) containing 0.1 M TBAP from 0 V to 1.4 V at a scan rate of 100 mVs^{-1} on (a) ITO electrode, (b) ZnO-coated ITO electrode

Fig. 5 exhibits CV curves of PTBTPA, ZnO and PTBTPA/ZnO composite film in DCM/ACN (7:3, by volume) containing 0.1 M TBAP as supporting electrolyte from 0 V to 1.4 V at a scanning rate of 50 mVs^{-1}. The inset depicts the enlarged view of CV curve for the ZnO film. The obvious redox peak of PTBTPA, PTBTPA/ZnO composite film and no redox peak in the curve of ZnO indicate that PTBTPA plays a dominant role in electrochromism of the whole composite system. The pure PTBTPA film displays a main oxidation peak at 1.07 V and a main reduction peak at 0.70 V with a difference of 0.37 V. While the PTBTPA/ZnO composite film shows a main oxidation peak at 1.04 V and a main reduction peak at 0.71 V with a difference of 0.33 V. The smaller margin between the oxidation potential and the reduction potential reflects the enhanced charge-transfer kinetics, the better reversibility of electrochemical reaction and more excellent cycle stability performance [45]. Therefore, it is expected that the core/shell composite incorporating PTBTPA with porous ZnO nanosheets would realize good electrochemical and electrochromic performance.

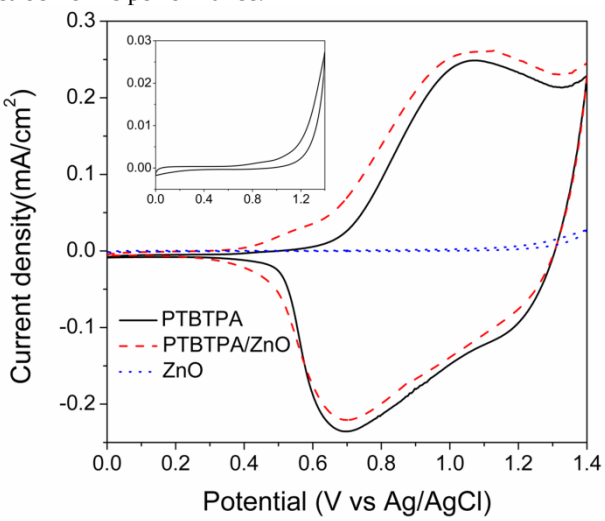

Fig. 5 Cyclic voltammogram curves of PTBTPA, ZnO nanosheets (inset: the enlarged curve) and PTBTPA/ZnO composite film recorded in DCM/ACN solutions (7: 3, by volume) containing 0.1 M TBAP at a scan rate of 50 mVs^{-1}

Fig. 6 depicts the UV–vis absorbance spectra of PTBTPA and PTBTPA/ZnO composite film under various applied potentials at 0 V, 0.9 V and 1.2 V. A well-defined maximum absorption band centered at 445 nm of PTBTPA (Fig. 6a) should be attributed to the π-π^* transition of the polymer backbone at the neutral state [46], and it decreases with the increase of potential. Besides, the appearance of charge carrier bands (at around 710 nm and 1100 nm) can be ascribed to the evolution of polaron and bipolaron bands. From Fig. 6b, the corresponding maximum absorption peak of PTBTPA/ZnO composite film locates at 460 nm and it also decreases with the increase of potential. The maximum absorption peak of PTBTPA/ZnO composite film at the neutral state emerges red-shift appearance of 15 nm compared to that of PTBTPA. The band gap values (*Eg*, calculated by using $Eg = 1240/\lambda_{onset}$; λ_{onset}: the onset value of the absorption.) of PTBTPA film and PTBTPA/ZnO composite film are 2.22 eV and 2.10 eV, respectively. Therefore, the core/shell composite system has the

lower energy gap due to the introduction of porous ZnO nanosheets with small nanoparticles [47], which would contribute to improve the electrochromic performance of polymer.

The PTBTPA film presents a multicolor electrochromism with orange in the reduced state (0 V), olive green in the middle state (0.9 V) and dark gray in the oxidized state (1.2 V), respectively (Fig. 6c). According to the color-displaying principle, the absorption wavelength is complementary to the displaying color. An absorption band centered at 445 nm of PTBTPA at 0 V is corresponding to orange, the absorption band centered at 710 nm at 0.9 V is corresponding to green, and multiple absorption peaks at 1.2 V is corresponding to gray due to the complementary effect of different colors. The absorption peak of PTBTPA/ZnO composite film emerges a little offset, but the color-displaying do not change substantially and it also exhibits three colors (orange, olive green and dark gray) (Fig. 6d). Therefore, ZnO nanosheets introduced into the PTBTPA film still preserves its original multicolor display performance.

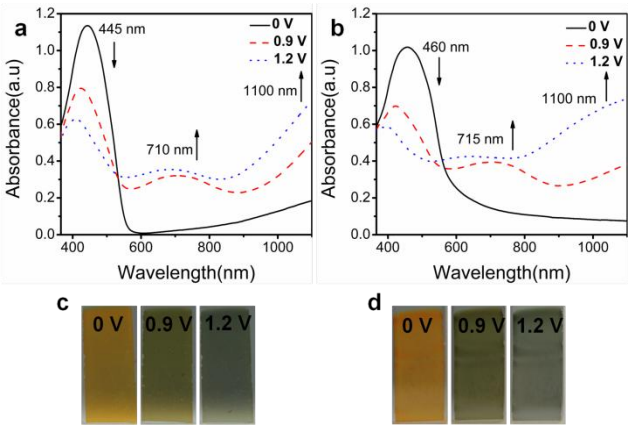

Fig. 6 Spectroelectrochemical spectra and color changes of (a, c) PTBTPA film, (b, d) PTBTPA/ZnO composite film in applied potentials of 0 V, 0.9 V and 1.2 V in DCM/ACN solutions (7:3, by volume) containing 0.1 M TBAP

The electrochromic switching behaviors of PTBTPA and PTBTPA/ZnO composite film are monitored at the maximum absorption in order to characterize their optical contrasts. Fig. 7 shows the optical contrasts and the switching times of PTBTPA film and PTBTPA/ZnO composite film, which are carried out between 0 V and 1.4 V with a residence time of 5 s (or 10 s) in the near NIR region (at 1100 nm). PTBTPA film shows optical contrasts of 51.2% (5 s), 51.8% (10 s) at 1100 nm (Fig. 7a). PTBTPA/ZnO composite film presents optical contrasts of 67.8% (5 s), 68.7% (10 s) for the relative wavelength (Fig. 7b). Obviously, the optical contrasts of the polymer and composite films have no great variation as the switch time increasing from 5 s to 10 s. However, the optical contrast of the composite film in near NIR region is enhanced by 17% compared to that of PTBTPA film. The switching time is defined as the time required for reaching 95% of the full change in absorbance after the switching of the potential. The switching time of PTBTPA film is 1.65 s at 1100 nm (Fig. 7c), while the switching time of PTBTPA/ZnO composite film is 0.96 s for the same wavelength (Fig. 7d). The result illustrates that the composite film has much faster switching speed than that of PTBTPA film. The reasons is summarized as follows: on one hand, porous ZnO nanosheets with loose inner space can facilitate counterions penetration into the polymer film and provide higher doping levels, devoting to the higher optical contrast; on the other hand, the core/shell composite structure can result in the shorter diffusion distance and faster counterion diffusion during the redox process, leading to the faster switching speed.

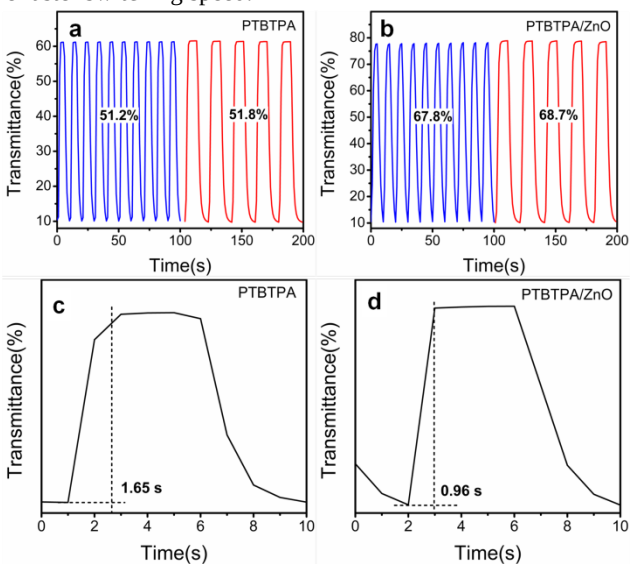

Fig. 7 Optical contrasts and switching response time of (a) PTBTPA film and (b) PTBTPA/ZnO composite film monitored at 1100 nm in DCM/CAN solutions (7:3, by volume) containing 0.1 M TBAP between 0 and 1.4 V with a residence time of 5 s and 10 s

Fig. 8 shows electrochemical impedance spectra of PTBTPA and PTBTPA/ZnO composite films in DCM/ACN (7:3, by volume) containing 0.1 M TBAP as supporting electrolyte. Generally, the impedance spectra consist of an intercept at the Z' axis, a semicircle in high frequency regions and a straight line in low frequency regions. In the impedance plot, the intercept at the Z' axis in high frequency corresponds to the resistance of the electrolyte (Re) between the working electrode and the counter electrode. The semicircle at impedance frequencies represents the charge transfer resistance (Rct), which is inner resistance of the film. The straight line at low frequencies reflects the diffusion resistance of the electrolyte to the electrode. From Fig. 8, the semicircle diameter of PTBTPA/ZnO composite electrode is 34.3 Ω, which is much lower than 82.9 Ω of PTBTPA electrode. The result demonstrates that PTBTPA/ZnO composite film has much lower inner resistance of the film. Therefore, it can be concluded that incorporating PTBTPA with ZnO nanosheets can facilitate counterions transport in the polymer film, which leads to higher optical contrasts and faster switching speed.

The electrochemical stability of EC materials toward long-term switching between the neutral and oxidized states is one of the most important factors for the application of EC devices [48]. Fig. 9 presents the stability curves of PTBTPA and PTBTPA/ZnO composite films between 0 V and 1.3 V for 1000 cycles in DCM/ACN (7:3, by volume) containing 0.1 M TBAP at a

scanning rate of 300 mVs-1. The CV curve of PTBTPA (Fig. 9a) reveals the film retaining 44% (after 500 cycles), 21% (after 1000 cycles) of its original electroactivity. However, the PTBTPA/ZnO composite film retained 86% (after 500 cycles), 70% (after 1000 cycles) of its original electroactivity (Fig. 9b). The result implies that the composite film has better redox stability and would be as a promising candidate material for EC devices. The main reason for the enhanced stability is that the polymer film covers outer surface of the ZnO nanosheets to form the core/shell structure, in which the nanosize ZnO grains anchor the polymer firmly on the substrate. Accordingly, the porous structure and inner small particles allow the excellent adhesion of the polymer to the substrate and prevent electrode from delaminating under repeated CV scanning. The enhanced interface adhesion between PTBTPA and the electrode could greatly increase the long-term stability of the polymer film.

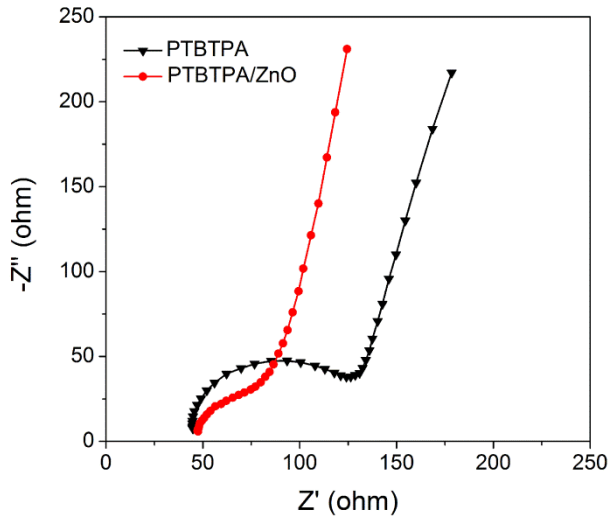

Fig. 8 Electrochemical impedance curves of PTBTPA film and PTBTPA/ZnO composite film

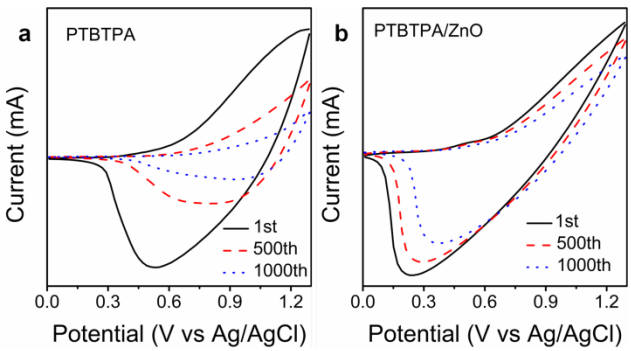

Fig. 9 Long-term stability of (a) PTBTPA film (b) PTBTPA/ZnO composite film as a function of repeated scans in DCM/CAN solutions (7:3, by volume) containing 0.1 M TBAP between 0 and 1.3 V. Scan rate: 300 mV s^{-1}

4. Conclusions

Porous ZnO nanosheets with PTBTPA core/shell composite were successfully prepared via electrodeposition and electropolymerization techniques. The composite film exhibits noticeable electrochromism with reversible color changes from orange (0V), olive green (0.9 V) and dark gray (1.2 V). An optical contrast of 68.7% and a switching time of 0.96 s are obtained for the composite film, better than that of the pure PTBTPA film, 51.8% and 1.95 s. The cyclic stability studies reveal that the composite film exhibits much more enhanced durability and retains 70% of the electroactivity even after 1000 cycles. However, the pure PTBTPA film loses almost most of its electroactivity after 1000 cycles. Our work confirms that porous ZnO nanosheets incorporated with conjugated polymer can effectively improve the electrochromic performances, which has important significance for the study of composite electrochromic system.

Acknowledgements

Financial support for this work was provided by the supporting of National Natural Science Foundation of China (51203138, 51273179), National Basic Research Program of China (2010CB635108, 2011CBA00700), International S&T Cooperation Program, China (2012DFA51210), Major Science and Technology.

Notes and references

State Key Laboratory Breeding Base of Green Chemistry-Synthesis Technology, College of Chemical Engineering and Materials Science, Zhejiang University of Technology, Hangzhou, China. Fax: +86-571-88320929; Tel: +86-571-88320929; E-mail: czhang@zjut.edu.cn (Cheng Zhang), ouyang@zjut.edu.cn (Mi Ouyang)

1 R. J. Mortimer, A. L. Dyer and J. R. Reynolds, *Displays*, 2006, **27**, 2.
2 P. Somani, A. B. Mandale and S. Radhakrishnan, *Acta Mater.*, 2000, **48**, 2859.
3 U. Bulut and A. Cirpan, *Syn. Met.*, 2005, **148**, 65.
4 S. Varis, M. Ak, C. Tanyeli, I. M. Akhmedov and L. Toppare, *Eur. Polym. J.*, 2006, **42**, 2352.
5 Z. T. Li, Y. Zhang, A. L. Holt, B. P. Kolasa, J. G. Wehner, A. Hampp, G. C. Bazan, T. Q. Nguyen and D. E. Morse, *New J. Chem.*, 2011, **35**, 1327.
6 S. Duluard, A. C. Cochet, I. Saadeddin, A. Labouret, G. Campet, G. Schottner, U. Posset and M. H. Delville, *New J. Chem.*, 2011, **35**, 2314.
7 F. B. Koyuncu, E. Sefer, S. Koyuncu and E. Ozdemir, *Polymer*, 2011, **52**, 5772.
8 F. B. Koyuncu, S. Koyuncu and E. Ozdemir, *Org. Electron.*, 2011, **12**, 1701.
9 D. Kumar, *Eur. Polym. J.*, 1999, **35**, 1919.
10 C. L. Gaupp, D. M. Welsh, R. D. Rauh and J. R. Reynolds, *Chem. Mater.*, 2002, **14**, 3964.
11 K. X. Sheng, H. Bai, Y. Q. Sun, C. Li and G. Q. Shi, *Polymer*, 2011, **52**, 5567.
12 L. Zhao, L. Zhao, Y. X. Xu, T. F. Qiu, L. J. Zhi and G. Q. Shi, *Electrochimi. Acta*, 2009, **55**, 491.
13 A.C. Sonavane, A.I. Inamdar, D.S. Dalavi, H.P. Deshmukh and P.S. Patil, *Electrochimi. Acta*, 2010, **55**, 2344.
14 A. C. Sonavane, A. I. Inamdar, H. P. Deshmukh and P. S. Patil, *J. Phys. D: Appl. Phys.*, 2010, **43**, 315102.

15 J. H. Zhu, S. Y. Wei, M. J. Alexander, T. D. Dang, T. C. Ho and Z. H. Guo, *Adv. Funct. Mater.*, 2010, **20**, 3076.
16 H. G. Wei, X. R. Yan, S. J. Wu, Z. P. Luo, S. Y. Wei and Z. H. Guo, *J. Phys. Chem. C*, 2012, **116**, 25052.
17 H. G. Wei, J. H. Zhu, S. J. Wu, S. Y. Wei and Z. H. Guo, *Polymer*, 2013, **54**, 1820.
18 G. F. Cai, J. P. Tu, D. Zhou, J. H. Zhang, X.L. Wang and C. D. Gu, *Sol. Energy Mater. Sol. Cells*, 2014, **122**, 51.
19 G. F. Cai, J. P. Tu, D. Zhou, J. H. Zhang, Q. Q. Xiong, X. Y. Zhao, X. L. Wang and C. D. Gu, *J. Phys. Chem. C*, 2013, **117**, 15967.
20 C. G. Wu, M. I. Lu and M. F. Jhong, *J. Polym. Sci. Pol. Phys.*, 2008, **46**, 1121.
21 W. J. Bae, A. R. Davis, J. Jung, W. H. Jo, K. R. Carter and E. B. Coughlin, *Chem. Commun.*, 2011, **47**, 10710.
22 S. Bhandari, M. Deepa, S. N. Sharma, A. G. Joshi, A. K. Srivastava and R. Kant, *J. Phys. Chem. C*, 2010, **114**, 14606.
23 Z. L. Wang and J. H. Song, *Science*, 2006, **312**, 242.
24 H. D. Yu, Z. P. Zhang, M. Y. Han, X. T. Hao and F. R. Zhu, *J. Am. Chem. Soc.*, 2005, **127**, 2378.
25 K. S. Choi, H. C. Lichtenegge and G. D. Stucky, *J. Am. Chem. Soc.*, 2002, **124**, 12402.
26 C. S. Lao, J. Liu, P. Gao, L.Y. Zhang, D. Davidovic, R. Tummala and Z. L. Wang, *Nano Lett.*, 2006, **6**, 263.
27 Y. Sun, G. M. Fuge, N. A. Fox, D. J. Riley and M. N. R. Ashfold, *Adv. Mater.*, 2005, **17**, 2477.
28 G. Z. Shen, Y. B. Bando, D. Liu, D. Golberg and C. J. Lee, *Adv. Funct. Mater.*, 2006, **16**, 410.
29 F. Li, Y. Ding, P. X. Gao, X. Q. Xin and Z. L. Wang, *Angew. Chem. Int. Ed.*, 2004, **43**, 5238.
30 X. W. Sun, J. X. Wang, Nano Lett., 2008, **8**, 1884.
31 M. Kateb, V. Ahmadi and M. Mohseni, *Sol. Energ. Mat. Sol. C.*, 2013, **112**, 57.
32 X. J. Lv, J. W. Sun, B. Hu, M. Ouyang, Z. Y. Fu, P. J. Wang, G. F. Bian and C. Zhang, *Nanotechnology*, 2013, **24**, 265705.
33 H. Chettah and D. Abdi, *Thin Solid Films*, 2013, **537**, 119.
34 J. H. Qiu, M. Guo, Y. j. Feng and X. D. Wang, *Electrochim. Acta*, 2011, **56**, 5776.
35 L. F. Xu, Q. W. Chen and D. S. Xu, *J. Phys. Chem. C*, 2007, **111**, 11560.
36 X. H. Lu, D. Wang, G. R. Li, C. Y. Su, D. B. Kuang and Y. X. Tong, *J. Phys. Chem. C*, 2009, **113**, 13574.
37 C. H. Chang, H. Jung, Y. Rheem, K. H. Lee, D. C. Lim, Y. Jeong, J. H. Lim and N. V. Myung, *Nanoscale*, 2013, **5**, 1616.
38 J. S. Cho , K. Uchida, N. Yoshioka and K. Yamamoto, *Sci. Technol. Adv. Mat.*, 2004, **5**, 697.
39 Q. Hou, L. Q. Zhu, H. N. Chen, H. C. Liu and W. P. Li, *Electrochim. Acta*, 2012, **85**, 438.
40 S. C. Ng, J. M. Xu , H. S. O. Chan, A. Fujii and K. Yoshino, J. Mater. Chem., 9 (1999) 381.
41 C. Li, T. Imae, *Macromolecules*, 2004, **37**, 2411.
42 S. H. Cheng, S. H. Hsiao, T. H. Su and G. S. Liou, *Polymer*, 2005, **46**, 5939.
43 M. Yang, G. S. Pang, J. X. Li, L. F. Jiang, D. X. Liang and S. H. Feng, *J. Phys. Chem. C*, 2007, **111**, 17213.
44 Y. Cao, Y. J. Tao, H. F. Cheng and Z. Y. Zhang, *J. Appl. Polym. Sci.* 2013, **129**, 3764.
45 V. H. Nguyen, E. M. Jin and H. B. Gu, *J. Power Sources*, 2013, **244**, 586.
46 C. Zhang, C. Hua, G. H. Wang, M. Ouyang and C. A. Ma, *Electrochim. Acta*, 2010, **55**, 4103.
47 M. Ahmad, E. Ahmed, Z. L. Hong, N. R. Khalid, W. Ahmed and A. Elhissi, *J. Alloy. Compd.*, 2013, **577**, 717.
48 X. Tu, X. K. Fu, Q. L. Jiang, Z. J. Liu, G. D. Chen, Dyes. Pigments, 2011, 88, 39.

Table of Contents (TOC)

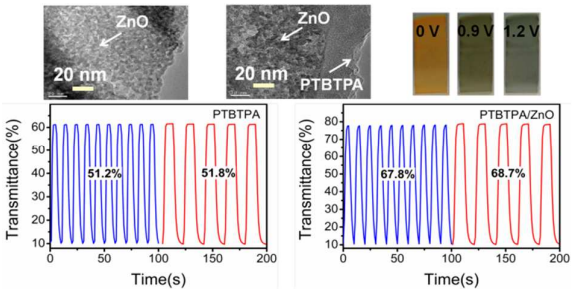

The core/shell composite film exhibits higher optical contrast, faster switching speed and better electrochemical stability.